Journal for ImmunoTherapy of Cancer

Novel banana lectin CAR-T cells to target pancreatic tumors and tumor-associated stroma

Mary K McKenna ,[1] Ada Ozcan,[1] Daniel Brenner,[2] Norihiro Watanabe,[1] Maureen Legendre,[3] Dafydd G Thomas,[4] Christopher Ashwood,[5] Richard D Cummings,[5] Challice Bonifant,[6] David M Markovitz,[3] Malcolm K Brenner[1]

To cite: McKenna MK, Ozcan A, Brenner D, *et al*. Novel banana lectin CAR-T cells to target pancreatic tumors and tumor-associated stroma. *Journal for ImmunoTherapy of Cancer* 2023;**11**:e005891. doi:10.1136/jitc-2022-005891

► Additional supplemental material is published online only. To view, please visit the journal online (http://dx.doi.org/10.1136/jitc-2022-005891).

Accepted 31 October 2022

[1]Center for Cell and Gene Therapy, Baylor College of Medicine, Houston, Texas, USA
[2]Department of Bioengineering, Rice University, Houston, Texas, USA
[3]Department of Internal Medicine, University of Michigan, Ann Arbor, Michigan, USA
[4]Department of Pathology, University of Michigan, Ann Arbor, Michigan, USA
[5]Department of Surgery, Harvard Medical School, Boston, Massachusetts, USA
[6]Department of Oncology, Sidney Kimmel Comprehensive Cancer Center, Johns Hopkins University School of Medicine, Baltimore, Maryland, USA

Correspondence to
Dr Mary K McKenna;
mary.mckenna@bcm.edu

ABSTRACT

Background Cell therapies for solid tumors are thwarted by the hostile tumor microenvironment (TME) and by heterogeneous expression of tumor target antigens. We address both limitations with a novel class of chimeric antigen receptors based on plant lectins, which recognize the aberrant sugar residues that are a 'hallmark' of both malignant and associated stromal cells. We have expressed in T cells a modified lectin from banana, H84T BanLec, attached to a chimeric antigen receptor (H84T-CAR) that recognizes high-mannose (asparagine residue with five to nine mannoses). Here, we tested the efficacy of our novel H84T CAR in models of pancreatic ductal adenocarcinoma (PDAC), intractable tumors with aberrant glycosylation and characterized by desmoplastic stroma largely contributed by pancreatic stellate cells (PSCs).

Methods We transduced human T cells with a second-generation retroviral construct expressing the H84T BanLec chimeric receptor, measured T-cell expansion, characterized T-cell phenotype, and tested their efficacy against PDAC tumor cells lines by flow cytometry quantification. In three-dimensional (3D) spheroid models, we measured H84T CAR T-cell disruption of PSC architecture, and T-cell infiltration by live imaging. We tested the activity of H84T CAR T cells against tumor xenografts derived from three PDAC cell lines. Antitumor activity was quantified by caliper measurement and bioluminescence signal and used anti-human vimentin to measure residual PSCs.

Results H84T BanLec CAR was successfully transduced and expressed by T cells which had robust expansion and retained central memory phenotype in both CD4 and CD8 compartments. H84T CAR T cells targeted and eliminated PDAC tumor cell lines. They also disrupted PSC architecture in 3D models in vitro and reduced total tumor and stroma cells in mixed co-cultures. H84T CAR T cells exhibited improved T-cell infiltration in multicellular spheroids and had potent antitumor effects in the xenograft models. We observed no adverse effects against normal tissues.

Conclusions T cells expressing H84T CAR target malignant cells and their stroma in PDAC tumor models. The incorporation of glycan-targeting lectins within CARs thus extends their activity to include both malignant cells and their supporting stromal cells, disrupting the TME that otherwise diminishes the activity of cellular therapies against solid tumors.

WHAT IS ALREADY KNOWN ON THIS TOPIC

⇒ In contrast to successful treatment of hematological malignancies, cell therapies for solid tumors have been thwarted by the hostile tumor microenvironment that impedes chimeric antigen receptor (CAR) T-cell activity. Novel therapies are required to overcome the antigen heterogeneity and stromal barriers present in solid tumors.

WHAT THIS STUDY ADDS

⇒ We have generated a novel lectin-based CAR T cell that can recognize malignant cells while also disrupting the supportive stromal cell component of solid tumors.

HOW THIS STUDY MIGHT AFFECT RESEARCH, PRACTICE OR POLICY

⇒ Banana lectin binds high-mannose glycans that are associated with the progression of multiple cancers. The use of H84T BanLec as a CAR T-cell targeting moiety broadens therapeutic activity with cytotoxicity against malignant cells and supporting stroma. This enhances antitumor activity for treatment of solid cancers.

INTRODUCTION

Cellular immunotherapies, including chimeric antigen receptor (CAR) T cells, have revolutionized the treatment of hematological malignancies. However, no CAR T cell has shown similar efficacy for the treatment of solid tumors. This limited success is attributed in part to the heterogenous and hostile tumor microenvironment (TME) that prevents access to malignant cells and adversely affects the survival and function of infiltrating effector cells. A lack of targetable tumor specific antigens that are also consistently expressed by malignant cells is an added major challenge.[1]

Altered glycosylation patterns are a hallmark of cancer.[2] Distinct from most tumor-associated antigens, cancer-associated glycans are found not only on tumor cells but also

on cellular stromal components of the TME,[3] making them ideal targets for immunotherapies. High-mannose glycans, which consists of five to nine mannose molecules covalently linked to an Asn residue, promote cancer progression and metastasis.[4–6] Moreover, distinct high-mannose glycosylation patterns are present on the tumor-associated stroma. This contrasts with distant normal stroma that has low abundance of high mannose.[6 7] Hence, abnormal glycan signatures are present on malignant cells and on adjacent supporting stroma. Targeting high-mannose residues should therefore both directly destroy malignant cells and disrupt the protective TME.

Lectins are proteins that, *inter alia*, recognize terminal sugars in glycoproteins with high specificity[8] and therefore represent a means of targeting the tumor glycome. We have designed a CAR derived from banana lectin (BanLec), an engineered lectin in which a single amino acid change, (histidine to threonine—H84T), uncoupled its mitogenicity from its glycan binding properties.[9] We chose to analyze the effects of T cells expressing this CAR targeted to pancreatic ductal adenocarcinomas (PDAC). This tumor has an intensely desmoplastic stroma contributed by pancreatic stellate cells (PSCs) that in normal pancreas are quiescent.[10] When activated in response to inflammation or tumor, PSCs proliferate and develop a myofibroblast phenotype. The resulting desmoplastic remodeling[11 12] limits the therapeutic T-cell infiltration likely required for effective cellular therapy.

Here, we describe how H84T CAR-T cells can directly target PDAC and also disrupt pancreatic stroma in vitro and in vivo. This dual mechanism thereby reduces tumor burden without reliance on consistent expression of a single antigen. The H84T CAR is one of the few CARs developed that targets tumor-specific glycans and is the first CAR driven by a lectin that shows in vivo efficacy.

RESULTS

Glycan profiling of PDAC tumors and PSCs

H84T BanLec binds high-mannose oligosaccharides[13] that are low or absent on normal mature cells. This property limits cross-reactivity with normal human, non-human primate, and rat tissues. Weak membrane staining was observed in rare leukocytes found in a few human tissues while the strongest staining was measured in cytoplasmic fractions of granulocytes and monocytes (SRI Biosciences Safety Report). This is consistent with high mannose branched N-glycans expressed on immature proteins before they are processed and reach the cell membrane, and therefore do not represent non-tumor specific targets for the lectin on the surface of healthy cells as confirmed by the lack of hematotoxicity seen when H84T BanLec was administered to rats[14] (Defense Biosciences Safety Report). By contrast, when we characterized the glycan profile of three different PDAC cell lines and primary PSCs by mass spectrometry (figure 1A and online supplemental figure 1), each cell line had unique glycan profiles but the CFPAC-1 and Capan-1 PDAC cell lines both expressed complex oligosaccharides, including targets for H84T. Panc-1 cells exhibited fewer complex saccharides compared with the other two tumor lines, with high mannose contributing to 85% of the expressed N-glycans. Primary PSCs exhibit more paucimannose compared with the other cell lines but high-mannose glycans were still the majority, contributing to over 75% of observed glycan intensity.

We confirmed that H84T BanLec could bind and recognize these high-mannose glycans by flow cytometry on all three PDAC cell lines and PSCs (figure 1B). By contrast, and consistent with earlier specificity analyses, H84T BanLec did not bind normal T cells which have a greater expression of complex sialylated N-glycans with only 40% of the observed glycan intensity being attributed to high-mannose N-glycans measured on PDAC cell lines. These data confirmed the binding specificity of H84T BanLec to malignant tumor and stroma cells while sparing normal cells.

Development of H84T CAR T cells

We investigated whether H84T BanLec could be used as a binder in a CAR and expressed in T cells, and whether the engineered cells would directly kill PDAC tumor lines. We cloned H84T into a second-generation CAR retroviral construct including an IgG4 short hinge region, CD28 transmembrane domain, 41BB costimulatory domain, and zeta chain (figure 2A). We tested other constructs with different costimulatory, hinge, and transmembrane domains, but this configuration ultimately provided the best ex vivo T-cell expansion. Therefore, we proceeded with functional testing of this transgenic H84T CAR construct. Following transduction, we detected stable surface expression on activated T cells of the H84T CAR using a custom H84T CAR specific antibody (mean expression: 70.9%±12.8%, n=6, figure 2B). During H84T CAR T-cell expansion in media supplemented with low concentrations of dasatinib (50 nM), there was no evidence of fratricide with H84T CAR T expanding identically to non-transduced (NT) controls (figure 2C). Analysis of T cell phenotype by flow cytometry confirmed retention of central-memory-like T cells ($CCR7^{+}CD45RA^{+}$) in both the CD4+ and CD8+ compartments (figure 2D,E).

Antitumor activity of H84T CAR T cells against PDAC tumor cell lines

We cultured H84T CAR T cells or NT control T cells with PDAC cell lines at effector to target ratios of 1:4. We measured residual viable tumor by MTS (3-(4,5-dimethylthiazol-2-yl)-5-(3-carboxymethoxyphenyl)-2-(4-sulfophenyl)-2H-tetrazolium) tetrazolium salt assay at 24 and 72 hours after T-cell addition (figure 3A, n=3 donors). Compared with cultures of target cells alone or with NT T cells, H84T CAR T cells significantly reduced viable tumor cells at 72 hours (CFPAC-1 p=0.001, CAPAN-1 p=0.003, Panc-1 p<0.0001). We confirmed H84T CAR T-cell targeting of tumor cells engineered to express GFP by assessing residual viable PDAC cell lines using flow

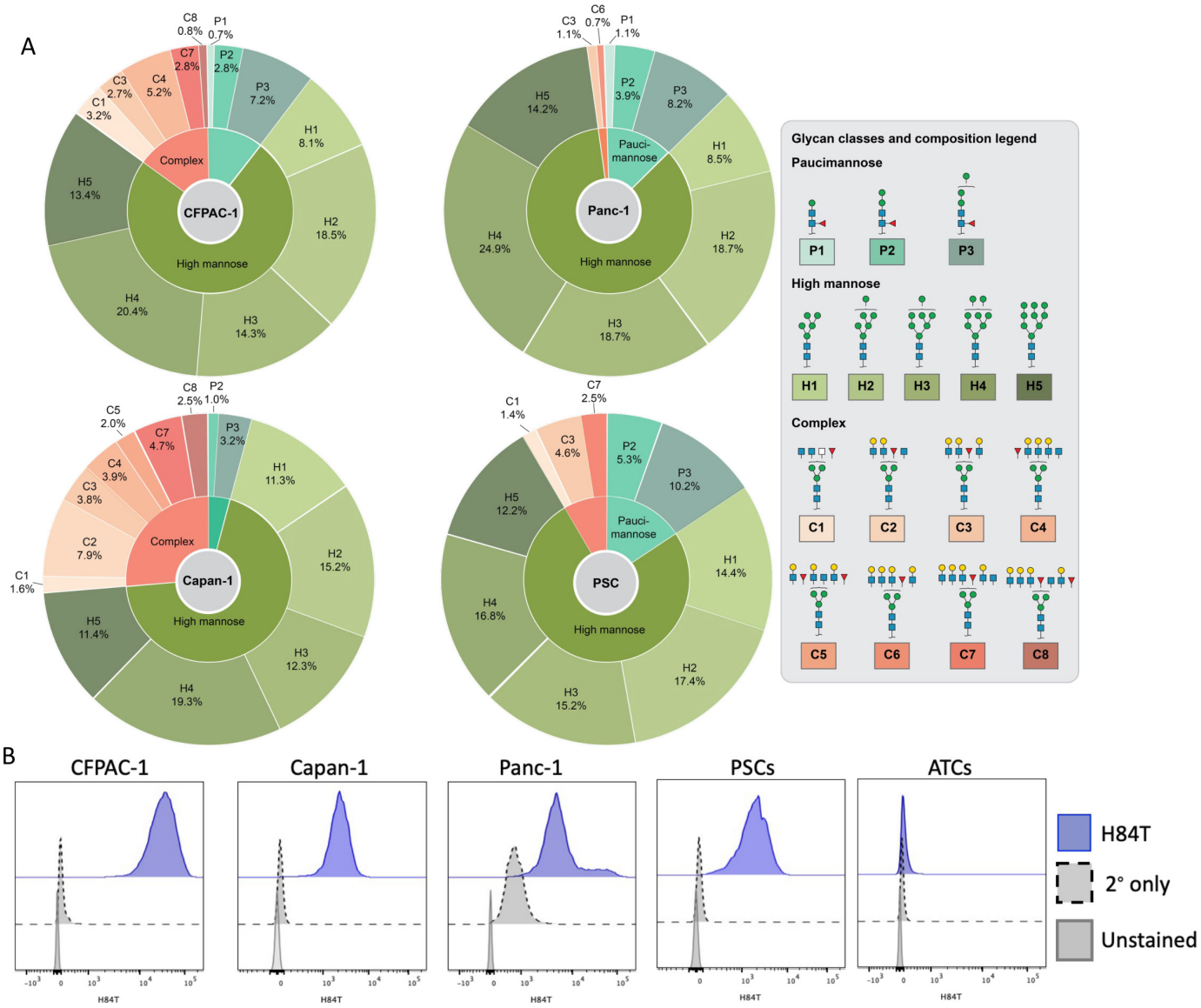

Figure 1 Glycan profile of PDAC tumor cell lines and primary PSCs. (A) Summary of N-glycan analysis by MALDI-TOF mass spectrometry for CFPAC-1, Panc-1, Capan-1, and PSCs. N-glycan profiling is described in detail in the methods section. (B) Cell surface detection of high-mannose expression by biotinylated H84T BanLec. PDAC tumor cells, PSCs, and activated T cells (ATCs) were stained with 0.4 µg/mL biotinylated H84T BanLec followed by APC streptavidin. Cells were stained with streptavidin alone (2° only) for control. Surface expression was analyzed by flow cytometry and mean fluorescent intensity is represented on histogram plots. BanLec, banana lectin; PDAC, pancreatic ductal adenocarcinoma; PSC, pancreatic stellate cells.

cytometric measurement of total GFP+7-AAD- cells with quantitative beads 24–96 hours after T-cell addition at an effector to target ratio of 1:4 (figure 3B, n=3 donors). Tumor cell death in these co-cultures at 72 hours corresponded to an increased T-cell expansion (online supplemental figure 2). H84T CAR T cells also secreted greater than two logs higher interferon (IFN)-γ after co-culture with all three PDAC cell lines than did NT control T cells at both 24 and 72 hours (figure 3C).

Activity of H84T CAR T cells against PSCs

The hostile environment of the PDAC stroma is a major impediment to treatment with CAR T cells and other cellular therapies. Primary PSCs are a major component of the desmoplastic structure of PDACs. These PSCs can express branched mannose glycans at sufficient density for binding by biotinylated H84T BanLec (figure 1). Therefore, we measured the activity of H84T CAR T cells against primary PSCs in two-dimensional (2D) co-culture at an effector to target ratio of 1:4. In contrast to H84T CAR T-cell co-cultures with PDAC tumor cells, we observed no significant cytotoxicity by H84T CAR T cells against PSC in either the MTS or flow cytometry assays (figure 4A,B). There was, however, evidence of H84T CAR T activation given that culture with PSCs stimulated increased IFN-γ secretion as compared with PSC culture with NT T cells (figure 4C). Thus, PSC appears to express

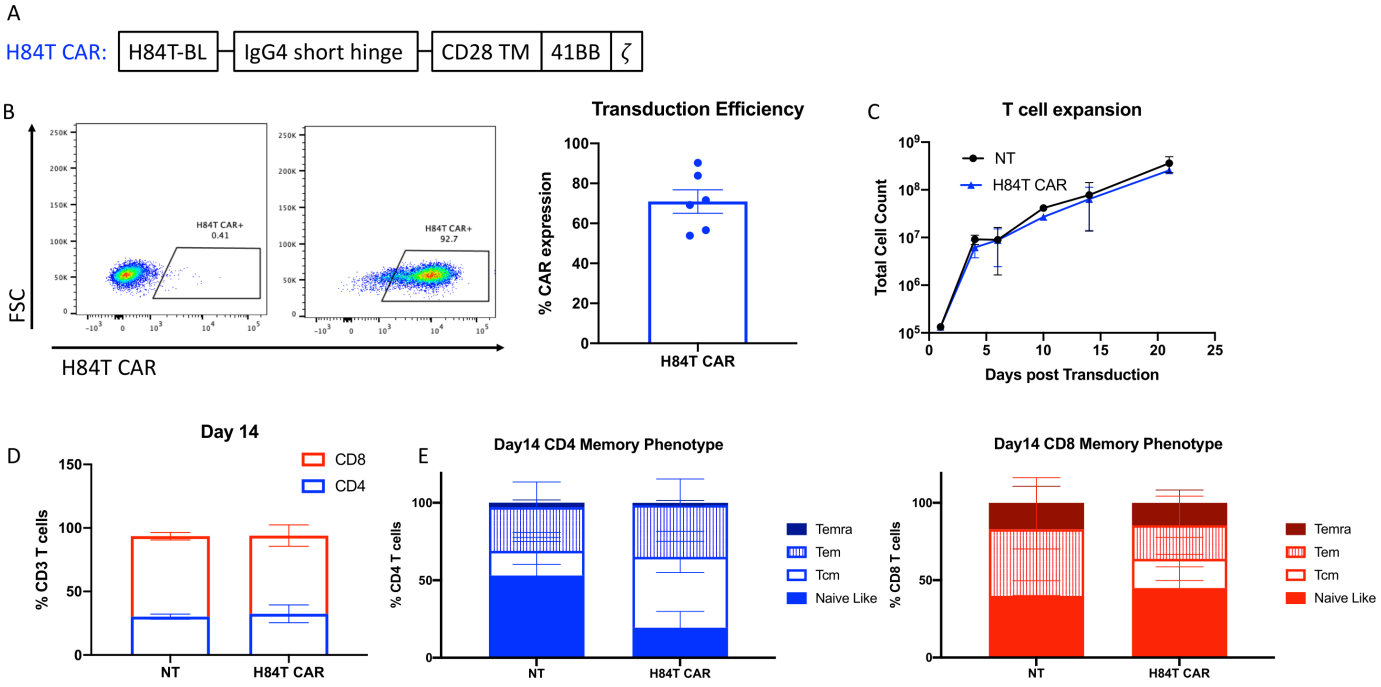

Figure 2 H84T CAR T-cell development. (A) Schematic diagram of retroviral CAR construct expressing H84T banana lectin binder with intracellular 41BB costimulatory domain and CD3z signaling domain. (B) H84T CAR expression was determined by flow cytometry with a rabbit anti-H84T antibody and goat anti-rabbit IgG Alexa Fluor 488 secondary antibody. Representative staining of one donor is shown in the plots on the left (left: non-transduced T cells; right: H84T CAR transduced). The average of six healthy donor T-cell transductions is quantified as percent CAR expression. (C) Average of five T-cell donor counts post transduction calculated by trypan blue counts. (D) Non-transduced (NT) and H84T CAR T cell CD4:CD8 ratio on day 14 post transduction quantified by flow cytometry. (E) Day 14 T-cell memory phenotype for CD4 (left) and CD8 (right) T cells. Memory T-cell populations were determined by cell surface expression of CCR7 and CD45RA staining quantified by flow cytometry. CAR, chimeric antigen receptor; Tcm, central memory; Teff, T effector cells; Temra,T cell effector memory.

sufficient target glycans to activate H84T cells, but insufficient to trigger target cell killing.

To investigate the potential for H84T CART activation mediated by the PSC stromal elements to disrupt tumor architecture, we used a three-dimensional (3D) in vitro model.[15] PSCs alone form spheroids within 24 hours. After CSFE (carboxyfluorescein succinimidyl ester) staining to label the cells with green fluoresence, we used an Incucyte Live imaging device to track GFP intensity in PSC spheroids over time in the presence of H84T CAR or control T cells (1:4 effector to target ratio). H84T CAR T cells disrupted the overall 3D architecture (figure 4D) of PSC spheroids leading to diffuse and significantly reduced GFP intensity (figure 4E, p<0.001). To determine if effector cell signaling following CAR engagement was required to disrupt the PSC architecture and infiltrate spheroids, we generated truncated H84T CAR T cells (H84TΔ) that lacked the CD3z intracellular signaling domain. We confirmed that H84TΔ T cells showed reduced phospho-CD3z expression compared with full-length H84T CAR T cells by flow cytometry (online supplemental figure 3a). H84T signaling deficient CAR T cells marginally reduced the PSC signal compared with NT T cell controls, but less so than full-length H84T CAR T cells (online supplemental figure 3b). Similarly, PSC spheroids treated with H84T CAR T cells showed an increase in Annexin V expression compared with PSC spheroids treated with NT or H84TΔ T cells (online supplemental figure 3c). These results suggest that H84T CAR T cells can infiltrate, disrupt, and target the stromal barrier created by PSCs, providing a novel mechanism of targeting heterogenous PDAC tumors.

H84T CAR T cells target and destroy heterogenous PDAC tumors in 3D in vitro models

Histologically, PDAC tumors are comprised of up to 50–80% stroma cells.[16 17] Therefore, to determine the combined consequences of direct tumor cell killing and PSC perturbation by H84T CAR T cells we used both 2D and 3D cultures that were combinations of PDAC and PSC. In 2D cultures, irrespective of the presence of PSCs, H84T CAR T cells were able to reduce the overall viability of tumor cells and PSCs at 24, 48, and 72 hours post culture (figure 5A).

To test the effect of H84T CAR T cells in complex 3D tumor spheroid models, we generated tumor spheroids containing both tumor and PSCs. None of the PDAC cell lines (CFPAC-1, Capan-1, and Panc-1) were able to form tumor spheroids alone but addition of PSCs provided support for multicellular tumor spheroids (online supplemental figure 4). At a ratio of 4 PSCs to 1 tumor cell, we found that PDAC tumor cells could form consistent spheroids with all three target tumor cell lines.

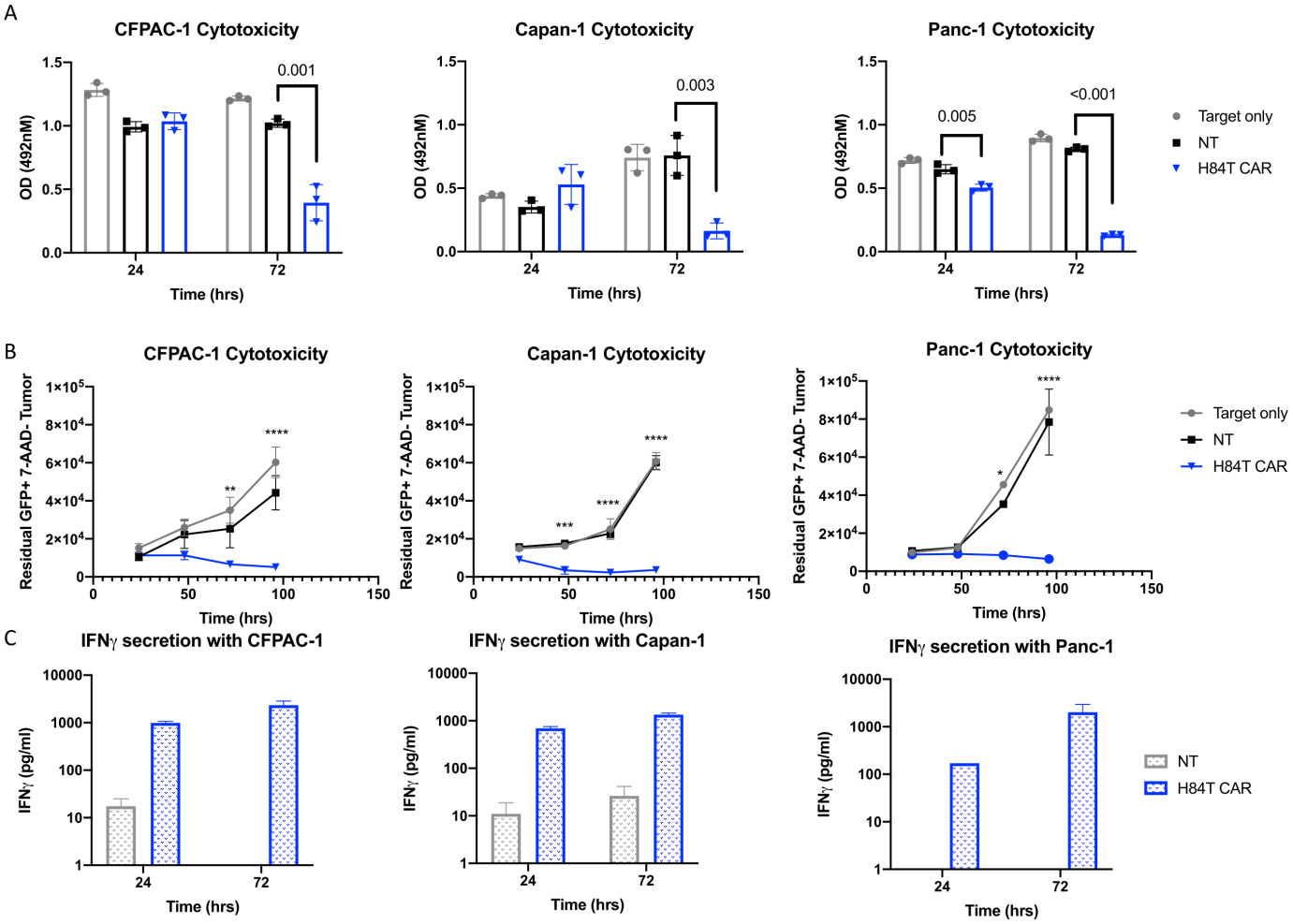

Figure 3 Antitumor activity of H84T CAR T cells against PDAC tumor cell lines. (A) 4×10^4 PDAC tumor cell lines were seeded in 96-well plates and 1×10^4 NT or H84T CAR T cells were added. Tumor cell viability was determined by MTS assay at 24 hours and 72 hours post T-cell addition. Optical density (OD) values were obtained at 492 nm wavelengths. Averages of three technical triplicates of three different donor T cells are represented. P values determined by unpaired student's t-test. (B) Co-culture of PDAC tumor cell lines with NT or H84T CAR T cells at a 4:1 ratio. Residual viable tumor cells labeled with GFP firefly luciferase were quantified by flow cytometry, 7-AAD staining and absolute counting beads. Samples were collected at 24, 48, 72, and 96 hours post T-cell addition. n=3–4 donors per cell line. P values determined by two-way analysis of variance comparing NT versus H84T; *p<0.05; **p<0.005;***p<0.0005; ****p<0.0001. (C) Supernatant from PDAC tumor cell lines cultured with NT or H84T CAR-T cells were collected 24 and 72 hours post T-cell addition (1:4 effector:target ratio). IFN-γ secretion was measured by ELISA assay. Average of three donors are represented. MTS, Tetrazolium Assay, 7-AAD; 7-aminoactionomycin D; CAR, chimeric antigen receptor; GFP;green fluorescent protein; IFN, interferon; PDAC, pancreatic ductal adenocarcinoma; NT, non-transduced.

Using Panc-1 cells labeled with GFP and unlabeled PSCs, we generated these mixed cellularity spheroids and added control NT or H84T CAR T cells at a 1:2 effector to tumor cell ratio and measured loss of GFP over time using Incucyte Live image analysis. H84T CAR T cells both reduced GFP intensity and disrupted spheroid structure compared with controls (figure 5B).

Since H84T CAR T cells could destroy the PSC spheroid stromal architecture (figure 4D), we investigated whether these effects modified H84T CAR T-cell infiltration of mixed tumor/stromal spheroids. CFPAC-1 tumor cells labeled with GFP were cultured with unlabeled PSCs at a ratio of 1:4. After 96 hours, NT and H84T CAR T cells were labeled with cell tracker red dye and added to spheroids at a 1:4 ratio of effector to tumor cells. We measured the mean RFP intensity under the brightfield mask of tumor and PSCs (online supplemental figure 5). H84T CAR T cells but not control T cells progressively infiltrated PDAC tumor+PSC spheroids for 48 hours and remained detected under the brightfield mask, suggesting that the activities of H84T CAR T cells allow penetration of PSC-contributed barriers in a PDAC tumor model (figure 5C, p<0.001). This is different from the activity that we observe with a conventional HER2 targeted CAR T cell that can only target tumor antigen but not PSCs (online supplemental figure 6). HER2 directed CARs have shown potent antitumor activity against solid tumors, including the PDAC that we are using in our studies (online supplemental figure 6A).[18 19] HER2 CAR T cells remain on the periphery of PSC spheroids (online supplemental figure

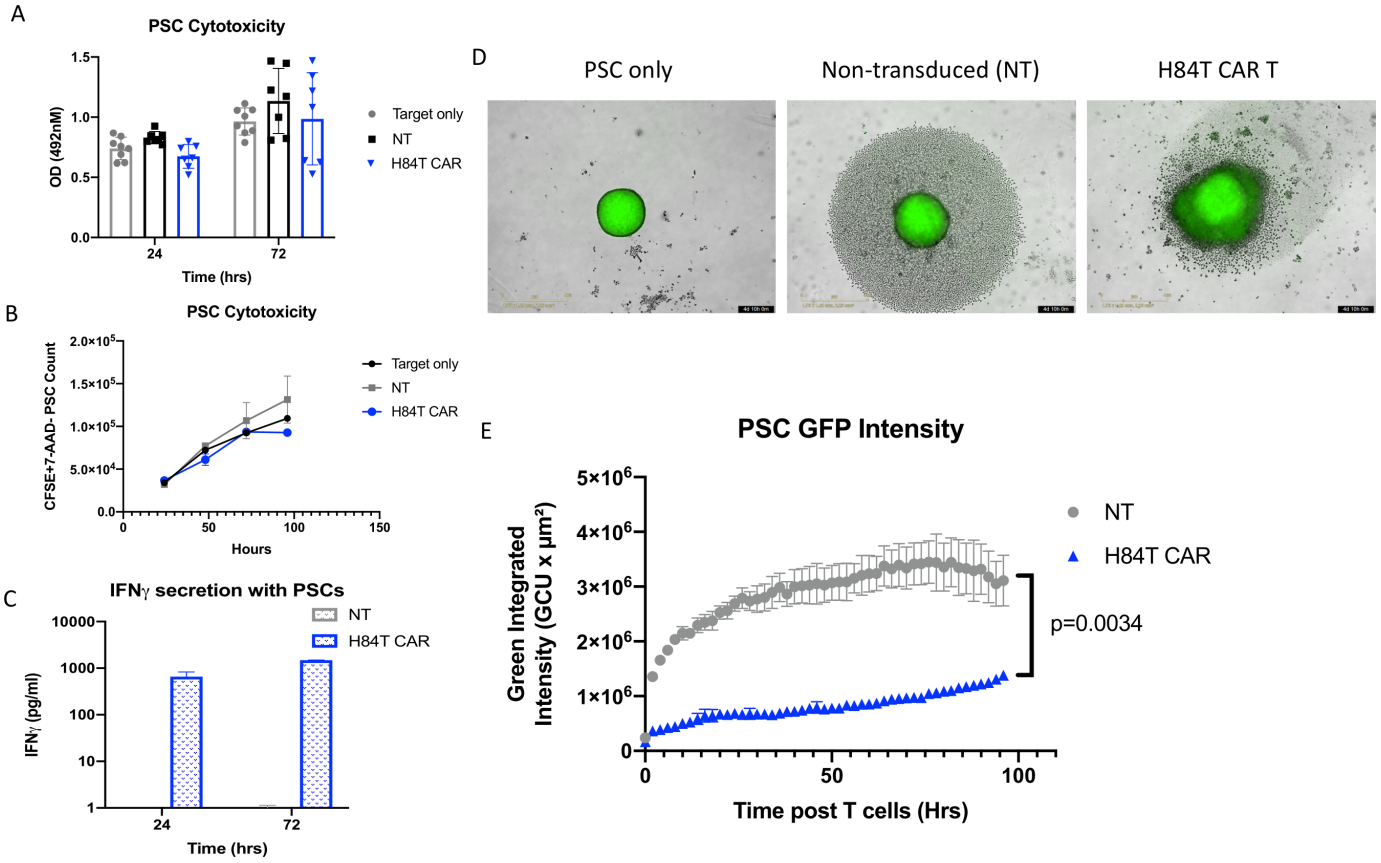

Figure 4 Anti-stromal activity of H84T CAR T cells against PSCs. (A) 4×10^4 primary PSCs were seeded in 96-well plates and 1×10^4 NT or H84T CAR T cells were added. PSC cell viability was determined by MTS assay at 24 hours and 72 hours post T-cell addition. Optical density (OD) values were obtained at 492 nm wavelengths. Averages of three technical triplicates of seven different donor T cells are represented. (B) Primary PSCs were stained with CSFE and cultured with NT or H84T CAR T cells are 4:1 ratio. Residual viable PSCs were detected by $CSFE^+7\text{-}AAD^-$ and quantified by absolute count bright beads via flow cytometry. (C) Supernatant from PSCs cultured with NT or H84T CAR-T cells were collected 24 and 72 hours post T-cell addition (1:4 effector:target ratio). IFN-γ secretion was measured by ELISA assay. Averages of three donors are represented. (D) 4×10^3 PSCs labeled with CSFE were seeded in 1% agarose coated 96-well plates and allowed to form spheroids for 24 hours. 2×10^3 NT or H84T CAR T cells were then added and images were acquired every 2 hours for 4 days by the Incucyte Live imaging system. Representative image of one donor T cell and spheroids is shown 96 hours post T-cell addition. (E) The green integrated intensity of CSFE labeled PSC spheroids were quantified by Incucyte Live image analysis post T-cell addition over time. Results are an average of four technical replicates of three different donors. P value determined by two-way analysis of variance. CSFE, Carboxyfluorescein succinimidyl ester; 7-AAD, 7-aminoactinomycin D; GFP, green fluorescent protein; CAR, chimeric antigen receptor; IFN, interferon; PSC, pancreatic stellate cells.

6B) and exhibit less infiltration in heterogenous tumor and PSC spheroids when compared with H84T CAR T cells (online supplemental figure 6C). These results confirm the unique ability of H84T CAR T cells to disrupt the PSC supportive architecture of PDAC tumors.

In vivo antitumor and anti-stromal activity of H84T CAR-T cells targeting heterogenous PDAC xenograft tumors

CFPAC-1 PDAC tumor cells labeled with GFP firefly luciferase (FfLuc) and PSCs were injected subcutaneously into NSG MHC KO mice. The tumors were monitored for 14 days until tumors reached an average volume of 40 mm^3. After a single injection of 1×10^6 NT or H84T CAR T cells, we monitored tumor signal via bioluminescence intensity and caliper measurements (figure 6A). H84T CAR T cells reduced the overall tumor signal compared with NT controls (figure 6B), which correlated with an overall reduced tumor volume (figure 6C). Tumor density was determined by ImageJ analysis of residual tumors on Day 42 post T-cell infusion (figure 6D). Representative H&E sections are shown in online supplemental figure 7.

GFP-FfLuc labeled NT and H84T CAR T cells were used to confirm H84T CAR T-cell homing to the primary tumor site with persistence greater than 30 days post infusion (figure 6E,F). In addition to efficacy against CFPAC-1 cells, antitumor activity of H84T CAR T cells was observed in reduced volume measurement of Panc-1 PDAC tumors (figure 6G). Similar antitumor activity was also observed with Capan-1 PDAC tumor cells co-injected with PSCs. Tumor volume and signal intensity were reduced in mice treated with H84T CAR T cells when compared with treatment with NT T cells (figure 6H,I, and online supplemental figure 8).

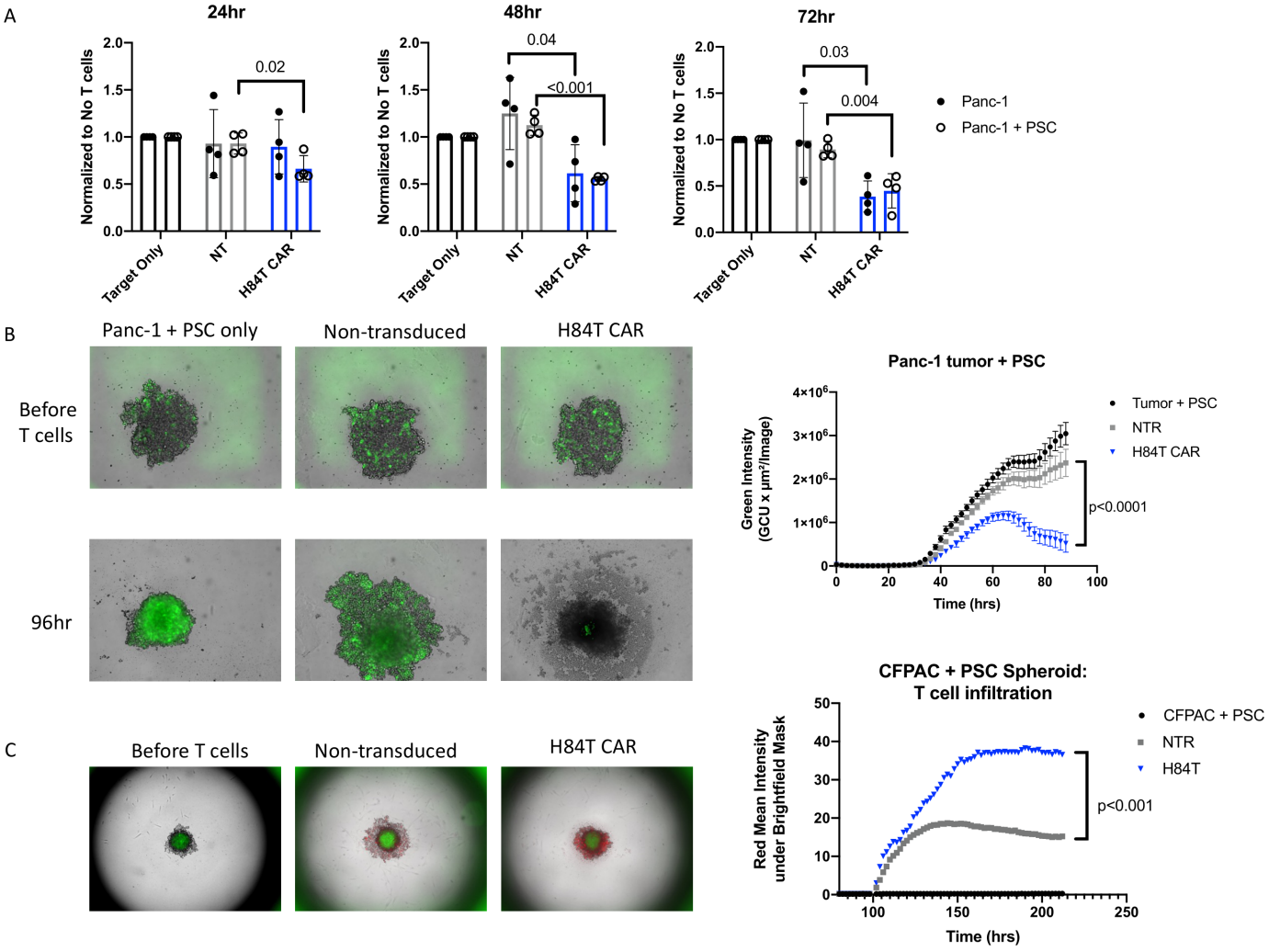

Figure 5 Activity of H84T CAR T cells in heterogenous pancreatic ductal adenocarcinoma tumor models. (A) 2×10^4 Panc-1 cells only or in combination with 2×10^4 PSCs were cultured for 24 hours in 96-well plates. 5×10^3 NT or H84T CAR T cells were then added and total viable tumor and PSCs were determined by MTS assay. Optical density was measured at 492 nm and tumor only control was normalized to 1. Measurements were acquired at 24 hours, 48 hours, and 72 hours post T-cell addition. (B) 2×10^3 GFP labeled Panc-1 tumor cells and 8×10^3 PSCs were co-cultured in 1% agarose coated 96-well plates for 48 hours. 1×10^3 NT or H84T CAR T cells were then added and imaged on the Incucyte Live imaging system for another 48 hours. GFP intensity of tumor cells was quantified over time (right) and representative images at time 0 hour and 96 hours post T cells are shown. P value<0.001 determined by two-way analysis of variance (ANOVA). (C) 2×10^3 GFP labeled CFPAC-1 tumor cells and 8×10^3 PSCs were co-cultured in 1% agarose coated 96-well plates for 96 hours. 1×10^3 NT or H84T CAR T cells labeled with cell tracker red were then added and spheroids were imaged every 2 hours on the whole well spheroid imaging setting. Spheroid images before T cells were added and 96 hours post T-cell addition is shown on the left. The red intensity of T cells quantified under the brightfield mask is graphed on the right (p<0.001 determined by two-way ANOVA). Quantification for determining T-cell signal within spheroids are further described in online supplemental figure 5 . CAR, chimeric antigen receptor; PSC, pancreatic stellate cells; NT, non-transduced; GFP, green fluorescent protein; MTS, MTS Tetrazolium assay.

To evaluate whether the beneficial antitumor effects of H84T CAR T cells in vivo were mediated in part by remodeling tumor stromal elements, we stained the CFPAC+PSC residual tumors on Day 42 with anti-human vimentin, a marker for stromal cells. Tumors treated with H84T CAR-T cells had reduced vimentin staining compared with tumors treated with NT T cells (figure 6E), consistent with H84T CAR T-cell disruption and reduction of the stromal component.

Finally, we observed no toxicity in any of the in vivo studies, an outcome consistent with the predicted lack of substantive cross-reactivity of the H84T binder with normal tissues, including normal pancreas (SRI Biosciences Safety Report).

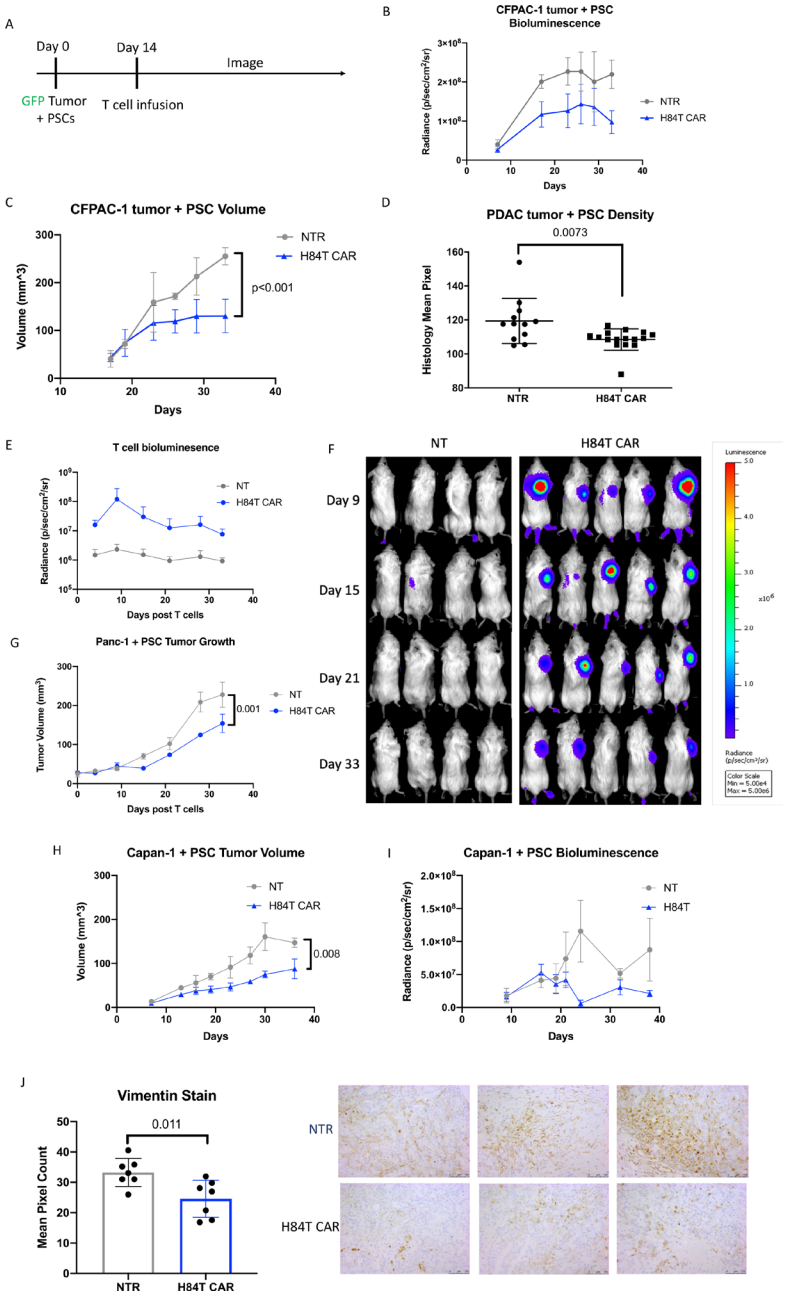

Figure 6 In vivo antitumor and anti-stromal activity of H84T CAR-T cells against three different PDACs. (A) NSG MHC KO mice were engrafted subcutaneously with 1×10^6 GFP-FfLuc labeled CFPAC-1 tumor cells and 1×10^6 PSCs. Tumors were allowed to establish for 2 weeks and then 1×10^6 NT or H84T CAR-T cells were intravenously delivered. (B) Tumor signal was quantified by bioluminescence signaling through IVIS imaging. N=4 mice per group. (C) Tumor volume was measured by the caliper and volume was calculated overtime. P value<0.001 determined by simple linear regression. (D) Residual tumors were resected on Day 36 post T-cell infusion and processed for H&E staining. Mean pixel density of H&E staining was quantified by ImageJ. Four sections per each tumor were quantified and graphed. N=3 tumors/NTR group and N=4 tumors/H84T group. P value determined by unpaired student's t-test. (E, F) NSG MHC KO mice were engrafted subcutaneously with 2×10^6 Panc-1 tumor cells and 2×10^6 PSCs. Tumors were allowed to establish for 2 weeks and then 1×10^6 NT or H84T CAR-T cells labeled with GFP-FfLuc were delivered intravenously. T-cell signal was quantified by bioluminescence signaling through IVIS imaging (F) bioluminesence images. (G) Tumor volume was measured by the caliper and volume was calculated overtime. N=4–5 mice per group. (H, I) NSG MHC KO mice were engrafted subcutaneously with 3×10^6 GFP-FfLuc labeled Capan-1 tumor cells and 3×10^6 PSCs. Tumors were allowed to establish for 1 week and then 1×10^6 NT or H84T CAR-T cells were intravenously delivered. Tumor volume (H) was quantified by caliper measurement and tumor signal (I) was quantified by bioluminescence signaling through IVIS imaging. N=4 mice per group. (J) Residual CFPAC-1+PSC tumors from mice treated with either NT or H84T CAR T cells were stained for anti-human vimentin to detect stroma cells. Vimentin pixel count was calculated by ImageJ analysis and representative IHC images are shown for three mice in each group. CAR, chimeric antigen receptor; PDAC, FfLuc, firefly luciferase; PDAC, pancreatic ductal adenocarcinoma; PSC, pancreatic stellate cells; NT, non-transduced; IHC, immunohistochemistry; GFP, green fluorescent protein.

DISCUSSION

We show that CAR T cells using a binder derived from an engineered BanLec (H84T) can recognize distinctive glycosylation patterns on both malignant PDAC cells and on the PSCs that form a major cellular component of their supporting stroma. Consequently, H84T CAR T cells can kill malignant cells directly and can facilitate CAR T-cell access to the interior of the tumor by disrupting the stromal barrier. This ability of a lectin-derived targeting element to simultaneously recognize heterogeneous patterns of tumor cell and stellate cell glycosylation helps address two major obstacles to successful immune cell therapy of pancreatic cancer, namely antigen heterogeneity and the hostile TME. Since aberrant patterns of glycosylation, including high-mannose residues, are widespread among many different tumor types, this approach may have application beyond pancreatic cancer.

Aberrant glycosylation has been associated with cancer progression for decades as it has been found to promote tumor cell proliferation, metastasis, and angiogenesis.[20] Tumor specific glycans have been a promising target for immunotherapies with monoclonal antibodies developed against tumor glycolipids such as the disialoganglioside GD2, leading to Food and Drug Administration approval of dinutuximab in 2015 for treatment of high-risk neuroblastoma.[21] However, the direct detection of glycan determinants has been difficult to develop as many carbohydrate associated glycan patterns are not immunogenic.[22] Of the available antibodies listed in the Database for Anti-Glycan Reagents (https://dagr.ccr.cancer.gov/About) only a fraction of them target different epitopes, with even fewer recognizing mannose molecules[23] considered to promote malignant progression of multiple tumors.[6 7 24] The lack of glycan specific antibodies has limited progress in targeting altered glycosylation patterns.[25] When such antibodies have been available, their application has been tumor restricted. Nevertheless, there is preclinical success of CAR T cells targeting cancer-specific antigen glycoforms of the Tn (Thomsen-nouveau) antigen and sialyl-Tn antigen expressed on cell membrane proteins such as mucin (Muc1).[26 27] Muc1 is an O-glycosylated protein that is aberrantly glycosylated at the Tn antigen site on multiple tumors including leukemia, breast, and pancreatic cancers.[28]

As an alternate to monoclonal antibody (scFv) derived targeting moieties, lectins have been substituted as CAR components that target glycosphingolipids such as Gb3, on multiple different cancer types including Burkitt's lymphoma, and colorectal and breast cancer cell lines.[29] Gb3 is expressed as multiple isoforms, which may limit discrimination between normal and malignant cells. By contrast, H84T BanLec, recognizes 5–9 mannose molecules covalently linked to asparagine residues of multiple proteins expressed on the surface of cancer cells. The majority of immature proteins expressing high-mannose glycans are normally cleaved in the Golgi before mature proteins are transported to the cell membrane, but this pathway is dysregulated in both cancer cells as well as tumor-associated stroma cells, such as the PSCs studied here.[4–7] This provides a unique target on both malignant cells and the tumor stroma recognized by H84T CAR T cells. Furthermore, because high-mannose glycans have minimal expression on normal cells, the specificity of H84T lectin and the CAR T cells derived therefrom should be high, with minimal on-target; off-tumor toxicities. Studies with the H84T lectin itself on human, non-human primate and rat tissues showed no binding to normal tissues/organs, including pancreas. Our own in vitro and in vivo studies with the H84T lectin and associated binder in a CAR T-cell supports the tumor specificity of H84T BanLec, with no toxicity from the H84T CAR T cells in our in vivo studies, with all mice maintaining both body weight and healthy body condition scores post T-cell infusion. Accurate assessment of safety and tolerability can only be accomplished in a clinical study, but should unexpected off target organ toxicity arise, there is precedence for successful modification of CAR expression or binders' affinity.[30 31] Like all exogenous proteins, H84T CAR-expressing T cells might be targeted by a host immune response.[32] Previous mouse studies showed that animals could indeed generate an antibody response to H84T BanLec, but these produced no functional inhibition.[33] Although we cannot predict the immune response to H84T CAR expressing T cells since our in vivo studies used immune-compromised animals with human tumor xenografts, these animals will partially mimic the human recipients of CAR T cells, in whom immune reactivity will be diminished by their tumor, its treatment and the standard lymphodepleting/cytoreductive chemotherapy given prior to all CAR T cell infusions.[34]

Targeting the tumor glycome by H84T CAR T may be particularly valuable given the impact of aberrant glycosylation of tumor antigens on the efficacy of conventional (scFv-based) CAR T-cell function.[35] Extracellular N-glycan abundance correlates with reduced CAR T-cell cytotoxicity as it inhibits effective immune synapse formation.[36] For example, the activity of CAR T cells directed to CD44v6 on pancreatic cancer could be improved by ablating α–1,6-mannosylglycoprotein 6-β-N-acetylglucosaminyltransferase 5, an enzyme involved in complex-type N-glycosylation of proteins or by treatment of the tumor with 2DG (2-deoxy-D-glucose), a glucose/mannose analog that disrupts N-glycan expression. Similarly, hyper-glycosylation of CD19 leads to antigen escape and CAR T-cell failure.[37] These two studies both suggest that suppressing aberrant glycosylation can improve CAR T-cell activity, and our approach that directly targets the glycome may ultimately be of complementary value, for example, in sequential or pulsed therapies that could overcome tumor glycome editing to escape one or other, but not both, of these therapeutic strategies.

While H84T CAR T cells were directly cytotoxic against PDAC tumor cell lines in conventional 2D co-culture assays (figure 3), in these same assays they had minimal direct cytotoxicity against PSCs despite the detection of high-mannose glycans, although at levels lower than for

the PDAC cells themselves (figure 1). Nonetheless, IFN-γ secretion by H84T CAR T cells cultured with PSCs indicated that interaction and activation through the H84T CAR had indeed occurred, since a similar phenomenon was not observed with NT T cells (figure 4). To better establish the biological consequences of this apparently non-lytic CAR T activation, we used 3D PSC spheroids,[15 38] since such systems better mimic solid tumor characteristics including cell-to-cell interactions, nutrient gradients, polarity, cellular ECM (Extracellular Matrix) composition and overall structure.[39] Moreover, studies culturing breast cancer cells in 2D versus 3D environments found substantive differences in N-glycosylation patterns[40] that may be sufficient to modulate the consequences of an interaction between a lectin CAR and its potential target. Similarly, studies in gastric cancer showed higher glycan expression in 3D multicellular spheroids compared with 2D cultures.[41] Importantly, when comparing the composition of N-glycans there was little difference between 3D models and human tumor xenografts or primary human (gastric) carcinomas,[41] suggesting 3D models better mimic the glycan structures on the surface of tumors in vivo compared with 2D cultures. Finally, PSCs are known to alter their phenotype when cultured in 3D systems, an effect that is accentuated when cultured with PDAC tumor cell lines.[42] Consistent with these precedents, the effects of H84T CAR T cells were more striking in 3D than in 2D cultures. The compact spheroidal 3D cultures, formed when PSCs are cultured alone or in combination with PDAC cells, were disrupted in the presence of H84T BanLec CAR T, resulting in a diffused and degraded spheroid architecture (figures 4 and 5). We observed that full-length CAR induces greater PSC cell death and disruption of PSC spheroids compared with the truncated H84T, suggesting that while a limited antitumor effect (spheroid disruption) is obtained following binding of the truncated CAR, maximal antitumor activity requires both receptor binding and effector T-cell activation. The improved ability of H84T CAR T cells to infiltrate the combined PDAC and PSC spheroids shown in figure 5C is a result consistent with their vitiated structure and will in turn expose more malignant cells and PSC to CAR T-cell targeting, a 'virtuous circle' of tumor disruption and destruction. Our in vivo xenograft models produced responses consistent with the observed ex vivo effects, with biopsied materials showing both a reduction in vimentin positive stromal cells and reduced tumor density and volume (figure 6). H84T CAR showed similar antitumor activity in all three PDAC and PSC xenograft tumor models tested with consistent tumor volume measurements.

H84T BanLec CAR can be expressed on the surface of natural killer cells that were found to mediate SARS-CoV-2 clearance.[43] We have now confirmed that we can indeed express H84T BanLec CAR on T cells and present the first report of a CAR T-cell guided by a lectin with antitumor activity in vivo, thus representing a new paradigm for CAR T development against cancer.[44] H84T CAR T cells provide a dual mechanism of action against solid tumors that has not been previously described. The ability to simultaneously target both malignant cells and their supporting tumor stromal elements allows us to improve T-cell infiltration and facilitate targeting of the malignant cells themselves. Moreover, the use of a lectin CAR that targets patterns of glycosylation present on many solid tumors but lacking on normal cells[4–7] (absent chronic inflammation or adjacent tumor), may allow H84T CAR activity to be widely inclusive of diverse human solid tumors, producing equity of outcome.

METHODS

Cells and culture condition

PDAC cell lines, CFPAC-1, Capan-1, and Panc-1, were obtained from ATCC (Manassas, Virginia, USA). GFP-FfLuc expressing cell lines were generated by gamma retroviral transduction with PG13 vector packaging cell line. Primary PSCs were obtained from ScienCell Research Laboratories. PSCs were used between the third and eighth passages and cultured in Stellate Cell Media and in tissue culture treated flasks treated with poly-L-lysine. Panc-1 tumor cell line was maintained in Dulbecco's modified Eagle's medium (supplemented with 10% fetal bovine serum (FBS) (GE Healthcare Life Sciences, Marlborough, Massachusetts, USA) and 2 mmol/L L-glutamine. CFPAC-1 and Capan-1 cells were maintained in Iscove's modified Dulbecco media (complete with 10% or 20% FBS, respectively). All cell lines were routinely tested for mycoplasma using the MycoAlert detection kit (Lonza; Basal, Switzerland).

N-glycan analysis

Purification of protein *N*-glycans was performed using standard protocols available through The National Center for Functional Glycomics website (www.ncfg.hms.harvard.edu). In brief, cells were lysed via probe sonication, and the cellular proteins were reduced by 10 mM DTT (DithioThreitol), alkylated by 55 mM iodoacetamide, and peptides obtained by overnight trypsin digestion. N-glycans were released from the tryptic peptides by overnight digestion with PNGase-F at 37°C. Released N-glycans were purified from intact proteins by C18 flow-through.

N-glycan permethylation was performed using a fresh slurry of NaOH/DMSO (Sodium Hydroxide/Dimethyl sulfoxide) and iodomethane mixed with the dried N-glycans. After the mixture became white, semi-solid and chalky, H_2O was added to stop the reaction and dissolve the sample. Chloroform:water liquid–liquid extractions were performed to remove residual salts and the chloroform fraction (containing the permethylated glycans) was then evaporated by vacuum centrifugation. Permethylated N-glycans were further desalted by C18 Sep-Pak (50 mg) according to the manufacturer's protocols.

For MALDI-TOF (Matrix-assisted laser desorption/ionization-time of flight mass spectrometry) analysis,

permethylated N-glycans were resuspended in 50% acetonitrile, mixed 1:1 with DHB (2,5-Dihydroxybenzoic acid) matrix and spotted on a metal 384 spot target plate. Spectra from the samples were obtained in a Bruker MALDI-TOF instrument using FlexControl Software in the reflection positive mode with a mass/charge (m/z) range of 1000–6000. Ten independent captures (representing 1000 shots each) were obtained from each sample.

CAR T-cell generation

Healthy normal donors gave informed consent to participate to donate peripheral blood mononuclear cells (PBMCs) through an Institutional Review Board-approved protocol. PBMCs were isolated using Lymphoprep according to manufacturer's instructions (Axis-Shield PoC AS, Dundee, Scotland). T cells were activated in 24-well non-tissue culture-treated plates coated with OKT3 (1 mg/mL; Ortho Biotech, Bridgewater, New Jersey, USA) and NA/LE anti-human CD28 antibodies (1 mg/mL; BD Biosciences, San Jose, California, USA) at a density of 1×10^6 cells per well. H84T CAR-T cells post transduction were expanded in conventional CTL media (45% RPMI-1640 media (HyClone Laboratories, Marlborough, Massachusetts, USA), 45% Click's medium (Irvine Scientific, Santa Ana, California, USA), 10% heat-inactivated FBS (HyClone Laboratories, Marlborough, Massachusetts, USA) and 2 mmol/L glutaMAX (Gibco by Life Technologies, Carlsbad, California, USA) supplemented with 10 ng/mL recombinant human interleukin (IL)-7 and IL-15 cytokines and 50 nM dasatinib to reduce tonic signaling and retain central memory CAR-T populations.[45 46]

H84T BanLec was cloned into the SFG (retroviral backbone) vector expressing IgG4 short hinge, CD28 transmembrane domain, 41BBz costimulatory domain, and CD3z signaling domain. H84TΔ retained the same extracellular binder without the 41BBZ and CD3z signaling domains. We performed transfection for retroviral supernatant with 293T cells and purified vector as described.[47] Retroviral transduction was performed as previously described.[18] Transduction efficiency of T cells was measured by flow cytometry after staining with a rabbit anti-H84T antibody generated in house at 1 µg/mL for 30 min, washed and then stained with 2 µg/mL Alexa Fluor 488 Goat anti-rabbit IgG (Jackson ImmunoResearch, Cat 111-545-144).

The vector encoding the HER2 directed CAR (second-generation HER2.28z; clone FRP5) was a kind gift from Dr Stephen Gottschalk. Transduction efficiency was measured by flow cytometry using a chimeric Erb2-Fc fusion protein (R&D Systems, Minneapolis, Minnesota, USA) with AF-647 anti-Fc antibody (Southern Biotech, Birmingham, Alabama, USA).

Flow cytometry

PDAC tumor cell lines, primary PSCs, and activated T cells were stained with biotinylated H84T lectin to recognize high-mannose glycan expression. Cells were stained with 0.4 µg/mL biotinylated H84T BanLec followed by APC streptavidin. Cells were stained with streptavidin alone (2° only) for control.

H84T CAR expression was described in the previous section. Both NT and H84T CAR T cells were stained for CD4, CD8, CCR7, and CD45RA (BD Biosciences, San Jose, California, USA) to determine T-cell memory phenotype.

Phospho-CD3ζ staining was performed by fixation in 2% formaldehyde at room temperature for 10 min. Cells were washed in phosphate-buffered saline (PBS) supplemented with 2% FBS followed by incubation with 100% cold methanol for 20 min at 4°C. Cells were then washed three times with PBS+2% FBS and stained with CD247 (Invitrogen, Waltham, Massachusetts, USA). Data were acquired on a BD CANTO II flow cytometer for all assays and data analyzed using FlowJo software.

Cytotoxicity assays

H84T CAR T and NT T cells were co-cultured with CFPAC-1, Capan-1, Panc-1 cell lines or PSC cell lines expressing GFP (or CSFE stained PSCs) at a 1:4 (effector to target) ratio. Residual tumor and PSCs were measured by GFP+7-AAD- staining quantified by flow cytometry and CountBright Absolute Counting Beads (Invitrogen by Thermo Fisher Scientific, Carlsbad, California, USA). For MTS (a colorimetric method) assays, tumor cells and T cells were seeded in the same ratio in a 96-well plate (2×10^4 tumor: 5×10^3 T cells). Viability of tumor cells was assessed at indicated time points by removing all supernatants from each well. 10 µL of CellTiter 96 AQueous One Solution (Promega, Madison, Wisconsin, USA) + 90 µL of media were then added to each well and incubated for 1 hour at 37°C. The optical density was then measured at 492 nm. For 2D cultures of both PDAC and PSCs together, cancer cells and PSC were seeded at a 1:1 ratio. T cells were added at a 1:4 effector to target ratio to the tumor cells only. MTS assay was performed as described to determine total viable tumor and PSCs remaining after T-cell addition.

IFN-γ ELISA

Tumor and PSCs were seeded in the same co-culture experiments for cytotoxicity studies. Supernatant was collected 24 and 72 hours after T-cell addition and analyzed for IFN-γ secretion (R&D Systems, Minneapolis, Minnesota, USA) according to the manufacturer's protocol.

3D spheroid assays

96-well tissue culture plates were coated with 1% agarose to create a low-attachment binding surface to allow forced suspension of tumor cells as described previously.[48 49] We seeded 2×10^3 tumor cells in 50 µL and PSCs were then added at different ratios to tumor in 50 µL volume. Cells were imaged until spheroids formed spontaneously and confirmed by microscope visualization. Studies determined that 2×10^3 tumor and 8×10^3 PSCs were required for spheroid formation 48 hours post cell addition. 1×10^3 NT or H84T CAR T cells were then added to spheroids.

Spheroids were monitored by Incucyte Live cell image analysis. If Annexin V was used for apoptosis detection, AF594 Annexin V (Invitrogen by Thermo Fisher Scientific, Carlsbad, California, USA) stain was used at 1:2000 dilution. Multispheroid protocol was used for image acquisition and quantified by the total red object integrated intensity parameter that represents the summed pixel intensity in calibrated units. For T-cell infiltration assay, NT or H84T CAR T cells were labeled with CellTracker Red (Invitrogen by Thermo Fisher Scientific, Carlsbad, California, USA). GFP labeled tumor and unlabeled PSCs were set up in the same ratios as all other experiments. Whole well spheroid protocol was used for image acquisition. Red mean intensity was calculated by Incucyte imaging software specifically under the brightfield mask of the tumor spheroid as shown in online supplemental figure 3.

Xenograft mouse models

Breeder pairs of NOD.Cg-*Prkdc*^{scid} *H2-K1*^{tm1Bpe} *H2-Ab1*^{em1Mvw} *H2-D1*^{tm1Bpe} *Il2rg*^{tm1Wjl}/SzJ mice (NSG MHC KO, Stock No. 025216) were purchased from The Jackson Laboratory (Bar Harbor, Maine, USA) and bred in the Baylor College of Medicine animal facility. Female and male (12–16 weeks old) mice were used for experiments. All animal experiments were conducted in compliance with the Baylor College of Medicine IACUC (Protocol #AN-4758).

We injected 1×10^6 CFPAC-1 cells expressing FfLuc and 1×10^6 unlabeled PSCs subcutaneously without Matrigel. Tumors were allowed to establish for 2 weeks and then 1×10^6 NT or H84T CAR-T cells were delivered intravenously via tail vein. For the Capan-1 tumor model, we injected 3×10^6 Capan-1 cells expressing FfLuc and 3×10^6 unlabeled PSCs subcutaneously without matrigel and tumors were allowed to establish for 1 week until palpable. For the Panc-1 tumor model we injected 2×10^6 unlabeled Panc-1 cells with 2×10^6 unlabeled PSCs and tumors were allowed to establish for 2 weeks. NT or H84T CAR T cells were then infused (1×10^6) and tumor was monitored by Xenogen-IVIS Imaging System (Caliper Life Sciences, Hopkinton, Massachusetts, USA). For Panc-1 mice, NT or H84T CAR T cells transduced with GFP-FfLuc were delivered intravenously. Mice were injected intraperitoneally two times a week with D-luciferin (150 mg/kg), and signal intensity (Radiance) was measured as total photon/sec/cm^2/sr (p/s/cm^2/sr) after imaging for both 10 s and 1 min exposures.[50] For GFP-FfLuc labeled T-cell experiments, mice were imaged post T-cell infusion on day 0 and then two times a week for 3 min exposures for the remainder of the experiment. Tumor volume was measured by caliper and volume was calculated by length (mm) × length (mm) × width (mm) measurements. We collected and processed residual tumors that were sectioned and stained for H&E and vimentin IHC (Cell Signaling, (D21H3) XP Rabbit mAb #5741) by the Baylor Pathology Core.

Statistics

All statistical analyses used GraphPad Prism software. We employed unpaired two-tailed Student's t-test with Welch's correction to determine the statistical significance of differences between samples. Simple linear regression analysis and two-way analysis of variance with Tukey's multiple comparison test with an alpha value of 0.5 was used for time course studies to compare treatments. Simple linear regression was used for tumor growth curves to determine whether the slopes and intercepts are significantly different from one another. All numerical data are represented as mean with SD. Results were considered statistically significant when $p<0.05$.

Twitter Mary K McKenna @McKenna_PhD_BCM

Acknowledgements The authors thank the Baylor College of Medicine Pathology Core (HTAP) and Dr Patricia Castro for performing immunohistochemistry and H&E staining supported by NCI award P30 CA125123.

Contributors Conceptualization: MKM, DMM and MKB. Investigation: MKM, DB, AO and CA. Formal Analysis: MKM, AO and CA. Resources: CB, NW, ML and DGT. Writing—Original Draft: MKM. Writing—Review and Editing: MKM, DMM and MKB. Supervision: MKB. Funding Acquisition: RC and MKB. Guarantor: MKM.

Funding This project was supported by the National Heart, Lung, and Blood Institute of the National Institutes of Health under award number 5T32HL092332-17 supervised by Dr Helen Heslop, the National Cancer Institute under the award 5PO1CA094237-15 and the Cancer Preventative and Research Institute of Texas (CPRIT) under the award RP220666. RC was supported by NIH grant R24 GM137763.

Competing interests CB is a St. Baldrick's Foundation Scholar, has pending patent applications describing the use of engineered T and natural killer cells to enhance tumor targeting, including the use of H84T-BanLec effector cell targeting of SARS-CoV-2 and has received research funding from Merck Sharp & Dohme, Kiadis Pharma, and Bristol Myers Squibb. MKB is supported by National Cancer Institute Grants No. P50CA126752 and P01CA094237, by Stand Up To Cancer (SU2C)/American Association for Cancer Research (AACR) 604817 Meg Vosburg T-Cell Lymphoma Dream Team, and the Leukemia and Lymphoma Society. SU2C is a program of the Entertainment Industry Foundation administered by the AACR. MKB is a co-founder with equity: Allovir, Tessa Therapeutics and Marker Therapeutics. Scientific Advisory Boards: Bluebird Bio, Tessa Therapeutics, Marker Therapeutics, Allogene, Walking Fish, KUUR, Pharmaceuticals, Tscan, Poseida, Cell Genix and Turnstone Biologics. Royalties from Bellicum and Takeda. DMM was supported by a grant from the Forbes Institute of the Rogel Cancer Center at the University of Michigan and is an inventor on University of Michigan patents concerning H84T BanLec.

Patient consent for publication Not applicable.

Ethics approval This study involves human participants and was approved by Baylor College of Medicine institutional review board: Protocol H-45017—studies of immune responses to tumor and viruses in healthy and immunocompromised individuals. Participants gave informed consent to participate in the study before taking part.

Provenance and peer review Not commissioned; externally peer reviewed.

Data availability statement No data are available.

ORCID iD
Mary K McKenna http://orcid.org/0000-0002-2357-1733

REFERENCES

1 Wagner J, Wickman E, DeRenzo C, *et al*. CAR T cell therapy for solid tumors: bright future or dark reality? *Mol Ther* 2020;28:2320–39.
2 Vajaria BN, Patel PS. Glycosylation: a hallmark of cancer? *Glycoconj J* 2017;34:147–56.
3 Peixoto A, Relvas-Santos M, Azevedo R, *et al*. Protein glycosylation and tumor microenvironment alterations driving cancer hallmarks. *Front Oncol* 2019;9:380.
4 de Leoz MLA, Young LJT, An HJ, *et al*. High-mannose glycans are elevated during breast cancer progression. *Mol Cell Proteomics* 2011;10:M110.002717–2717.
5 Park DD, Phoomak C, Xu G, *et al*. Metastasis of cholangiocarcinoma is promoted by extended high-mannose glycans. *Proc Natl Acad Sci U S A* 2020;117:7633–44.
6 Ščupáková K, Adelaja OT, Balluff B, *et al*. Clinical importance of high-mannose, fucosylated, and complex N-glycans in breast cancer metastasis. *JCI Insight* 2021;6. doi:10.1172/jci.insight.146945. [Epub ahead of print: 22 Dec 2021].
7 Boyaval F, van Zeijl R, Dalebout H, *et al*. N-glycomic signature of stage II colorectal cancer and its association with the tumor microenvironment. *Mol Cell Proteomics* 2021;20:100057.
8 Mazalovska M, Kouokam JC. Plant-Derived lectins as potential cancer therapeutics and diagnostic tools. *Biomed Res Int* 2020;2020:1–13.
9 Swanson MD, Boudreaux DM, Salmon L, *et al*. Engineering a therapeutic lectin by uncoupling mitogenicity from antiviral activity. *Cell* 2015;163:746–58.
10 Ferdek PE, Jakubowska MA. Biology of pancreatic stellate cells-more than just pancreatic cancer. *Pflugers Arch* 2017;469:1039–50.
11 McCarroll JA, Naim S, Sharbeen G, *et al*. Role of pancreatic stellate cells in chemoresistance in pancreatic cancer. *Front Physiol* 2014;5:141.
12 Apte MV, Pirola RC, Wilson JS. Pancreatic stellate cells: a starring role in normal and diseased pancreas. *Front Physiol* 2012;3:344.
13 Swanson MD, Winter HC, Goldstein IJ, *et al*. A lectin isolated from bananas is a potent inhibitor of HIV replication. *J Biol Chem* 2010;285:8646–55.
14 Moremen KW, Molinari M. N-Linked glycan recognition and processing: the molecular basis of endoplasmic reticulum quality control. *Curr Opin Struct Biol* 2006;16:592–9.
15 McKenna MK*et al*. Mesenchymal stromal cell delivery of oncolytic immunotherapy improves CAR-T cell antitumor activity. *Mol Ther* 2021.
16 Apte MV, Park S, Phillips PA, *et al*. Desmoplastic reaction in pancreatic cancer: role of pancreatic stellate cells. *Pancreas* 2004;29:179–87.
17 Hwang RF, Moore T, Arumugam T, *et al*. Cancer-associated stromal fibroblasts promote pancreatic tumor progression. *Cancer Res* 2008;68:918–26.
18 Ahmed N, Brawley VS, Hegde M, *et al*. Human epidermal growth factor receptor 2 (HER2) -specific chimeric antigen receptor-modified T cells for the immunotherapy of HER2-positive sarcoma. *J Clin Oncol* 2015;33:1688–96.
19 Hegde M, Joseph SK, Pashankar F, *et al*. Tumor response and endogenous immune reactivity after administration of HER2 CAR T cells in a child with metastatic rhabdomyosarcoma. *Nat Commun* 2020;11:3549.
20 Munkley J, Elliott DJ. Hallmarks of glycosylation in cancer. *Oncotarget* 2016;7:35478–89.
21 Dhillon S. Dinutuximab: first global approval. *Drugs* 2015;75:923–7.
22 Thurin M. Tumor-Associated glycans as targets for immunotherapy: the Wistar Institute Experience/Legacy. *Monoclon Antib Immunodiagn Immunother* 2021;40:89–100.
23 Sterner E, Flanagan N, Gildersleeve JC. Perspectives on anti-glycan antibodies gleaned from development of a community resource database. *ACS Chem Biol* 2016;11:1773–83.
24 Scott DA, Norris-Caneda K, Spruill L, *et al*. Specific N-linked glycosylation patterns in areas of necrosis in tumor tissues. *Int J Mass Spectrom* 2019;437:69–76.
25 Reports funded by National Institutes of Health. Transforming glycoscience: a roadmap for the future the National academies collection 2012.
26 Posey AD, Schwab RD, Boesteanu AC, *et al*. Engineered CAR T cells targeting the cancer-associated Tn-Glycoform of the membrane mucin MUC1 control adenocarcinoma. *Immunity* 2016;44:1444–54.
27 He Y, Schreiber K, Wolf SP, *et al*. Multiple cancer-specific antigens are targeted by a chimeric antigen receptor on a single cancer cell. *JCI Insight*2019;4.
28 Tarp MA, Sørensen AL, Mandel U, *et al*. Identification of a novel cancer-specific immunodominant glycopeptide epitope in the MUC1 tandem repeat. *Glycobiology* 2007;17:197–209.
29 Winfried Römer AVM. Rubí M-H Velasco Cárdenas, Simon Lagies, LinA Siukstaite, Oliver S. Thomas, Wilfried Weber, Bernd Kammerer, Susana Minguet. *Novel lectin-based chimeric antigen receptors target Gb3-positive tumour cells. Cellular and Molecular Life Sciences* 2022.
30 Pulè MA, Straathof KC, Dotti G, *et al*. A chimeric T cell antigen receptor that augments cytokine release and supports clonal expansion of primary human T cells. *Mol Ther* 2005;12:933–41.
31 Ghorashian S, Kramer AM, Onuoha S, *et al*. Enhanced CAR T cell expansion and prolonged persistence in pediatric patients with all treated with a low-affinity CD19 CAR. *Nat Med* 2019;25:1408–14.
32 Baker MP, Reynolds HM, Lumicisi B, *et al*. Immunogenicity of protein therapeutics: the key causes, consequences and challenges. *Self Nonself* 2010;1:314–22.
33 Covés-Datson EM, King SR, Legendre M, *et al*. A molecularly engineered antiviral banana lectin inhibits fusion and is efficacious against influenza virus infection in vivo. *Proc Natl Acad Sci U S A* 2020;117:2122–32.
34 Okada S, Vaeteewoottacharn K, Kariya R. Application of highly immunocompromised mice for the establishment of patient-derived xenograft (PDX) models. *Cells* 2019;8. doi:10.3390/cells8080889. [Epub ahead of print: 13 Aug 2019].
35 Car T-cell efficacy in solid tumors is affected by N-glycosylation. *Cancer Discov* 2022;12:598.
36 Greco B, Malacarne V, De Girardi F, *et al*. Disrupting N-glycan expression on tumor cells boosts chimeric antigen receptor T cell efficacy against solid malignancies. *Sci Transl Med* 2022;14:eabg3072.
37 Heard A, Landmann JH, Hansen AR, *et al*. Antigen glycosylation regulates efficacy of CAR T cells targeting CD19. *Nat Commun* 2022;13:3367.
38 McKenna MK, Rosewell-Shaw A, Suzuki M. Modeling the Efficacy of Oncolytic Adenoviruses. In: *Vitro and in vivo: current and future perspectives*. 12. Basel, 2020.
39 Nunes AS, Barros AS, Costa EC, *et al*. 3D tumor spheroids as in vitro models to mimic in vivo human solid tumors resistance to therapeutic drugs. *Biotechnol Bioeng* 2019;116:206–26.
40 Mao Y, Zhao Y, Zhang Y, *et al*. In-depth characterization and comparison of the N-glycosylated proteome of two-dimensional- and three-dimensional-cultured breast cancer cells and xenografted tumors. *PLoS One* 2020;15:e0243789.
41 Balmaña M, Mereiter S, Diniz F, *et al*. Multicellular human gastric-cancer spheroids mimic the glycosylation phenotype of gastric carcinomas. *Molecules* 2018;23. doi:10.3390/molecules23112815. [Epub ahead of print: 30 Oct 2018].
42 Norberg KJ, Liu X, Fernández Moro C, *et al*. A novel pancreatic tumour and stellate cell 3D co-culture spheroid model. *BMC Cancer* 2020;20:475.
43 Christodoulou I, Rahnama R, Ravich JW, *et al*. Glycoprotein targeted CAR-NK cells for the treatment of SARS-CoV-2 infection. *Front Immunol* 2021;12:763460.
44 Raglow Z, McKenna MK, Bonifant CL, *et al*. Targeting glycans for CAR therapy: the advent of sweet cars. *Mol Ther* 2022;30:2881–90.
45 Zhang H, Hu Y, Shao M, *et al*. Dasatinib enhances anti-leukemia efficacy of chimeric antigen receptor T cells by inhibiting cell differentiation and exhaustion. *J Hematol Oncol* 2021;14:113.
46 Mo F, Watanabe N, McKenna MK, *et al*. Engineered off-the-shelf therapeutic T cells resist host immune rejection. *Nat Biotechnol* 2021;39:56-63.
47 Mamonkin M, Rouce RH, Tashiro H, *et al*. A T-cell-directed chimeric antigen receptor for the selective treatment of T-cell malignancies. *Blood* 2015;126:983–92.
48 Lv D, Hu Z, Lu L, *et al*. Three-dimensional cell culture: a powerful tool in tumor research and drug discovery. *Oncol Lett* 2017;14:6999–7010.
49 Thomsen AR, Aldrian C, Bronsert P, *et al*. A deep conical agarose microwell array for adhesion independent three-dimensional cell culture and dynamic volume measurement. *Lab Chip* 2017;18:179–89.
50 Hoyos V, Del Bufalo F, Yagyu S, *et al*. Mesenchymal stromal cells for linked delivery of oncolytic and apoptotic adenoviruses to non-small-cell lung cancers. *Mol Ther* 2015;23:1497–506.